J. Fluid Mech. (1968), *vol.* 33, *part* 3, *pp.* 545–560
Printed in Great Britain

Growth of spectral components in a wind-generated wave train

By ALEX J. SUTHERLAND

Department of Civil Engineering, Stanford University†

(Received 3 October 1967 and in revised form 19 February 1968)

Power spectral density measurements were made of the water surface displacement in a wind-generated wave train in the Stanford wind, water-wave research facility. Growth rates of different components were determined from the measured spectra. The resulting values were compared with those predicted by the viscous Reynolds stress mechanism of energy transfer from wind to wave which was proposed by Miles. Where the growth was exponential the theory could be made to predict growth rates successfully at wave frequencies less than 3·5 c/s. At higher frequencies the theory predicted values an order of magnitude larger than those measured. Limited regions of linear growth were found at the lowest wind speed for components with frequencies less than 2·5 c/s. The scatter in the data did not permit a quantitative comparison with theory to be made for this range.

1. Introduction

Interaction between a turbulent air flow and a water surface results in a transfer of energy from air to water with the subsequent generation of water waves. During the last decade there have been many advances towards a better understanding of the mechanisms involved in this air–water interaction. A summary of these developments is given by Phillips (1966) as part of an integrated treatise on the problems of air and sea interaction. About the wind-wave generation problem Phillips (1966) comments, '. . . it appears that theory and observation may at last be becoming mutually relevant'.

Theoretical papers by Miles (1957), Phillips (1957) and Benjamin (1959) provided the first analyses of the wind-wave problem. Later papers by Miles (1959, 1960, 1962*a*) presented alternative mechanisms for energy transfer, each of which is applicable under specified conditions. For example, the mechanism presented by Miles (1962*a*) requires the air-velocity profile to be linear with height at the critical layer. This is the elevation y_c at which the air velocity is equal to the wave celerity. Under these conditions the critical layer must be inside the viscous sublayer. If the sublayer thickness is $\delta = 5\nu/U_*$, where ν is the kinematic viscosity of air and U_* is the shear velocity, then one can show that $y_c < \delta$ if $c/U_* < 10$ where c is the wave celerity. In the Stanford facility when the waves are purely wind generated, c/U_* has a maximum value of approximately 9·0.

† Now at School of Engineering, University of Canterbury, Christchurch, New Zealand.

Accordingly, in the present investigation, the growth of various components in a wave spectrum is determined and compared with the growth predicted by Miles's (1962*a*) theory.

2. Theory

The theory, as proposed by Miles (1962*a*), considers two-dimensional wave motion in a slightly viscous liquid subjected to prescribed stresses at its surface. The liquid is assumed to be of depth d and surface tension is taken into account. Surface waves of amplitude a and wave-number k such that $ka \ll 1$ are considered. The prescribed normal and tangential stresses, which are produced at the interface by a parallel shear flow above the water surface, are calculated by following the method of Benjamin (1959). Solution of the problem for fluid motion beneath the interface, subject to boundary conditions which match the computed surface stresses, leads to an eigenvalue equation for the complex wave speed $c = c_r + ic_i$. The growth factor, $kc_i = m$, is found from solutions of this equation which are given for the case $s \ll 1$, where s is the ratio of the density of the upper fluid to that of the lower fluid.

Miles (1962*a*) defines a parameter $z = y_c(U_c'k/\nu)^{\frac{1}{3}}$, where U_c' is the velocity gradient at the critical layer and ν is the kinematic viscosity of the upper fluid. For $z \ll 1$ and if the effect of viscous damping in the lower fluid is negligible, then

$$m = skU_* \left\{ \frac{0{\cdot}332}{w^2} \left(\frac{U_*}{kv}\right)^{\frac{2}{3}} \frac{c_0}{U_*} + \frac{0{\cdot}343}{w} \left(\frac{U_*}{kv}\right)^{\frac{1}{3}} \right\}, \tag{1}$$

where c_0 is the deep-water wave celerity and w is a function dependent upon the velocity profile in the upper fluid. Miles (1962*a*) assumed a linear profile

$$U(y) = (U_*^2/\nu)y \quad \text{for} \quad 0 \leqslant y \leqslant y_1 \leqslant 1/k,$$

where y_1 is the sublayer thickness. For $y \geqslant y_1$ the profile is assumed to fair smoothly into the above and to be asymptotically logarithmic, i.e.

$$U(y) \sim U_1 + \frac{U_*}{\kappa}\left[\ln\frac{4\kappa U_* y}{\nu} - 1 + O(y/y_1)\right] = \frac{U_*}{\kappa}\ln\frac{U_* y}{\nu} + C, \tag{2}$$

where U_1 is the velocity at y_1 and κ is the von Kármán constant. For this profile

$$w = \frac{\kappa c}{U_*} W[R, A],$$

where $R = \kappa U_*/k\nu$ and $A = \kappa(U_1 - c_0)/U_*$. Numerical values of W have been tabulated (Miles 1962*b*).

Experimentally the growth rates are determined by means of the spectrum of surface displacement. Using the results of Miles (1960), Hidy & Plate (1966) show that the frequency spectrum expressed as a function of fetch F has the asymptotic form

$$\phi(\sigma, F) \sim \frac{\sigma^5}{\rho_w^2 g^4} \frac{\exp(4mF/c) - 1}{4m} \int_0^\infty \pi(k, t) \cos\sigma t \, dt, \tag{3}$$

where g is the gravitational acceleration, σ is the wave frequency, ρ_w is the water density and $\pi(k, t)$ represents the spectrum for turbulent pressure fluctuations in the air.

By differentiating (3) logarithmically with respect to F and assuming the integral to be independent of F, we find

$$\frac{\partial}{\partial F}\{\ln \phi\} = \frac{1}{c}\left\{\frac{4\exp(4mF/c)}{\exp(4mF/c)-1}\right\}\left[m + F\frac{\partial m}{\partial F}\right] - \frac{1}{m}\frac{\partial m}{\partial F}. \tag{4}$$

The quantity $S = \partial/\partial F\{\ln \phi\}$ will be referred to as the growth rate. If the variation of m with fetch is very small and $4mF/c > 5$ then (4) reduces to

$$\frac{\partial}{\partial F}\ln \phi = \frac{4m}{c}. \tag{5}$$

Referring back to (3) we see that if $4mF/c \ll 1$ then

$$\phi(\sigma, F) \sim \frac{\sigma^5}{\rho_w^2 g^4}\frac{F}{c}I = \frac{\sigma^6}{\rho_w^2 g^5}FI, \tag{6}$$

where I denotes the integral in (3). By assuming again that I is independent of fetch for a given wind condition the theory predicts that, for each frequency σ, ϕ increases linearly with fetch.

3. Experimental apparatus

The experimental measurements were made in the Stanford Hydraulic Laboratory's wind, water-wave facility the main section of which is a channel 115 ft. long with a rectangular cross-section 3 ft. in width and 6 ft. 4 in. in height. A glass-walled test section extends for approximately 70 ft. from the inlet section to a beach used to absorb wave energy and to reduce wave reflexions. A schematic representation of the channel together with the upstream and downstream conditions is given in figure 1.

Turning vanes and a wire screen, mounted in the curved air intake section, minimize the non-uniformity of the entering air stream. The flow is straightened by a 2 in. thick honeycomb as it enters the test section. An upstream beach was formed by a slightly sloping (approximately 1:100) smooth plate, 5 ft. in length, mounted with one end immediately downstream of and level with the base of the entrance honeycomb. Between the test section and the fan there is a $1\frac{1}{2}$ in. thick honeycomb used to straighten the flow and a 5 ft. long transition section. The air velocity is controlled by adjusting the fan speed. Further details on the design are given in the report by Sutherland (1967).

Time-average velocity profiles in the air stream were measured using a total head tube and a static pressure tube mounted 1 in. apart and parallel to each other on a traversing probe. Pressure differences between the two tubes were monitored by a Pace differential transducer, the voltage output from which was recorded on a Sanborn recorder and converted directly to air velocity by means of a calibration curve. Effects arising from the small changes in temperature and humidity during the experiments were found to be negligible.

Wave height measurements were made using surface-penetrating, capacitance-type wave gauges. Nyclad insulated wire, no. 36 HNC with diameter 0·06 in., formed the sensing element. Data were recorded on analogue tape, converted to

digital form and analysed using an IBM 7090 computer at the Stanford computation centre.

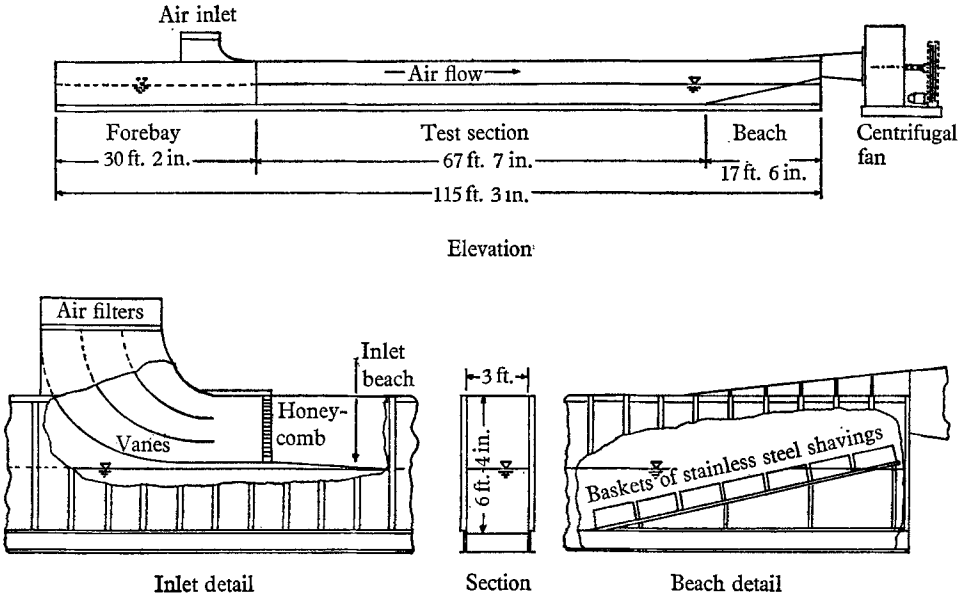

FIGURE 1. The Stanford wind, water-wave facility.

4. Computations

4.1. *Spectra*

Power spectra were computed, using the methods of Blackman & Tukey (1959), from the relation

$$\phi(\sigma) = \frac{2}{\pi}\int_0^\infty \overline{\eta(t)\,\eta(t+\tau)}\cos\sigma\tau\,d\tau,$$

where $\eta(t)$ is the water surface displacement, τ is a time lag and the overbar denotes the mean value. A smoothing (Hamming) process was used on the computed values. Most calculations were done with a Nyquist frequency f_{ny} of 16 c/s and some, at short fetches, with $f_{\mathrm{ny}} = 20$ c/s. The 80 % confidence band on each spectrum was estimated to be $+14\,\%$ and $-12\,\%$. The effect of a sharply peaked spectrum, which is to increase the width of the confidence band, was offset by repeating runs and averaging. The final results have an 80 % confidence band of approximately $\pm 12\,\%$. A frequency resolution of 0·333 c/s was used throughout.

4.2. *Growth rates from Miles's theory*

The velocity U_1 at the edge of the viscous sublayer must be known before the parameter A (see §2) can be evaluated. It is convenient to define $\alpha = U_1/U_*$ and thus

$$A = \kappa(\alpha - c_0/U_*).$$

To find α experimentally, the measured velocity profile, written as

$$u = \frac{U_*}{\kappa}\ln(y/z_0),$$

where z_0 is the elevation at which the logarithmic profile predicts zero velocity, must be equated to the asymptotic value of the profile assumed by Miles (1962*a*) and given in (2). However, from the resulting equation, it can be seen that to achieve values of $\alpha > 0$ we must have

$$z_0 U_*/\nu < 1{\cdot}68.$$

Invariably this limit is exceeded and α is computed to be negative, which is physically impossible.

Hidy & Plate (1966) overcame the above difficulty by assuming that U_1 is equal to the measured air velocity at an elevation equal to the standard deviation $(\overline{\eta^2})^{\frac{1}{2}}$ of the water surface displacement from the mean surface level. Values of α from their experiments ranged from 5·1 to 9·0. Miles (1962*a*) noted that for aerodynamically smooth flow over water there is evidence suggesting that the ratio $\alpha = U_1/U_*$ exceeds 6·6, which is the value found for flow over rough flat plates. This agrees with the values used by Hidy & Plate (1966). In this investigation α was treated as a free parameter and growth rates computed for $\alpha = 6$, 8 and 10.

Preliminary calculations were done to evaluate $\partial m/\partial U_*$ by first calculating m from (1) and then plotting it as a function of U_* for fixed values of k and α. The gradient of these curves, at the required values of U_*, defined $\partial m/\partial U_*$. Growth rates were then computed as follows. First, U_* was determined at fetches F_i from measured velocity profiles at $F = F_i$. The derivative $\partial U_*/\partial F$ was found by plotting these values as a function of fetch and fitting a straight line through the data points. Equation (1) was then used to find m at each F_i for the wave component of interest and a fixed value of α. The growth rates were then calculated from (4) for each F_i by using appropriate values of $\partial m/\partial U_*$ and $\partial U_*/\partial F$ to determine $\partial m/\partial F$. This method assumes that U_* is constant and equal to that at F_i for all fetches less than F_i and may be considered an improvement over calculating one growth rate based on a mean value of U_* at an intermediate fetch. Further refinements could be introduced into the computation: however, in view of the limited accuracy of the measured spectra, the writer feels that such an approach is not warranted.

5. Results

Four series of experiments were performed, each with a different mean air velocity. A reference air velocity U_0 was defined as the free-stream velocity at a fetch of 19·1 ft. and is shown in table 1. In each series velocity profiles were measured at six different stations and spectra of water surface displacement were determined at twelve stations ranging in fetch from 3·9 to 59·0 ft.

5.1. *Characteristics of the air flow*

The velocity profiles were not truly logarithmic, the lower portion tending to droop slightly towards the water surface, see figure 2. Such profiles introduce a degree of uncertainty into any values of surface stress determined from them. Hidy & Plate (1966), who also measured curved velocity profiles, determined the

surface stress by using a relation between the pressure gradient and the set-up at the water surface. Both these quantities are extremely small in the Stanford facility and thus subject to large errors in measurement. Further, since local values of surface stress were required for the computations detailed later, this method appeared to be unpractical.

Series	Reference air velocity, U_0 ft./s	Shear velocity U_* ft./s (fetch = 19·1 ft.)
I	22·0	1·67
II	31·0	2·63
III	39·0	3·40
IV	50·1	5·45

TABLE 1. Experimental conditions

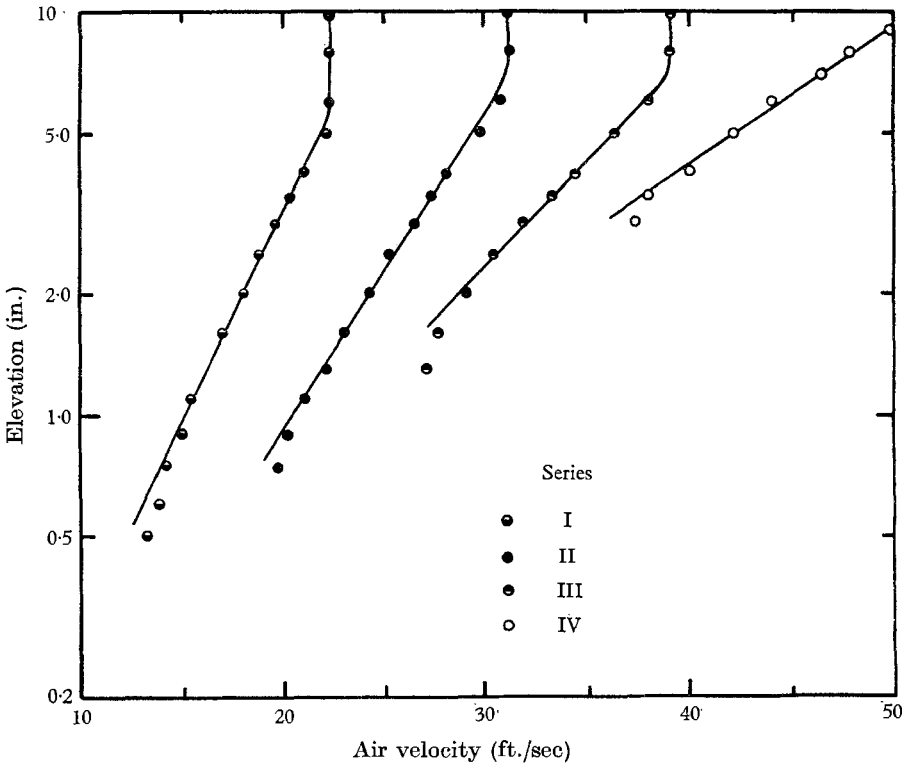

FIGURE 2. Air velocity profiles.

The least reliable velocity measurements are those made near the water surface where two effects can be important. First, the instantaneous velocities may differ over the crest and trough (Miles 1957) and, secondly, a fixed velocity probe is continuously changing streamlines. The former causes values larger than actual to be recorded while the latter causes recording of smaller values. Shemdin (1967) has shown that these effects can be significant at elevations less than three

times the wave amplitude. In view of this result the lowest points on the velocity profile were disregarded, the surface stress and thus U_* being determined from straight lines drawn through the remaining data. Examples are shown in figure 2.

Values of U_* increased monotonically with fetch. In each series the increase was approximately 10 %, the average over the length of the facility corresponding closely with that measured at a fetch of 19·1 ft. and shown in table 1.

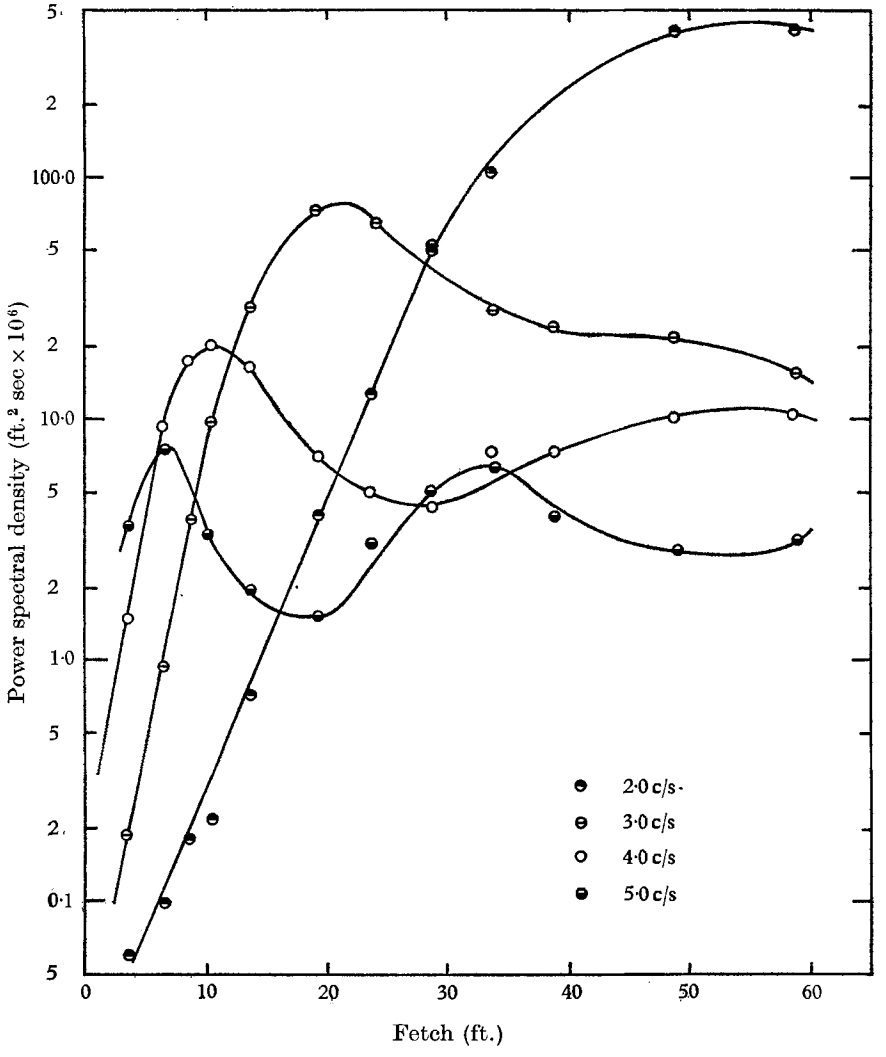

FIGURE 3. Growth of spectral components with fetch. Series III.

5.2. *Growth of spectral components*

The growth of a spectral component of frequency σ can be traced by plotting the spectral density $\phi(\sigma, F)$ as a function of fetch for a fixed wind velocity. Typical growth curves are shown in figure 3. The straight portions of each curve indicate regions of exponential growth as predicted by the theory when $4mF/c \gg 1$ and the

variation of m with fetch is small, see (5). Each frequency component reaches a maximum value of $\phi = \phi_{\max}$. Since viscous dissipation has a greater effect on high-frequency waves, the balance between energy input and dissipation will be

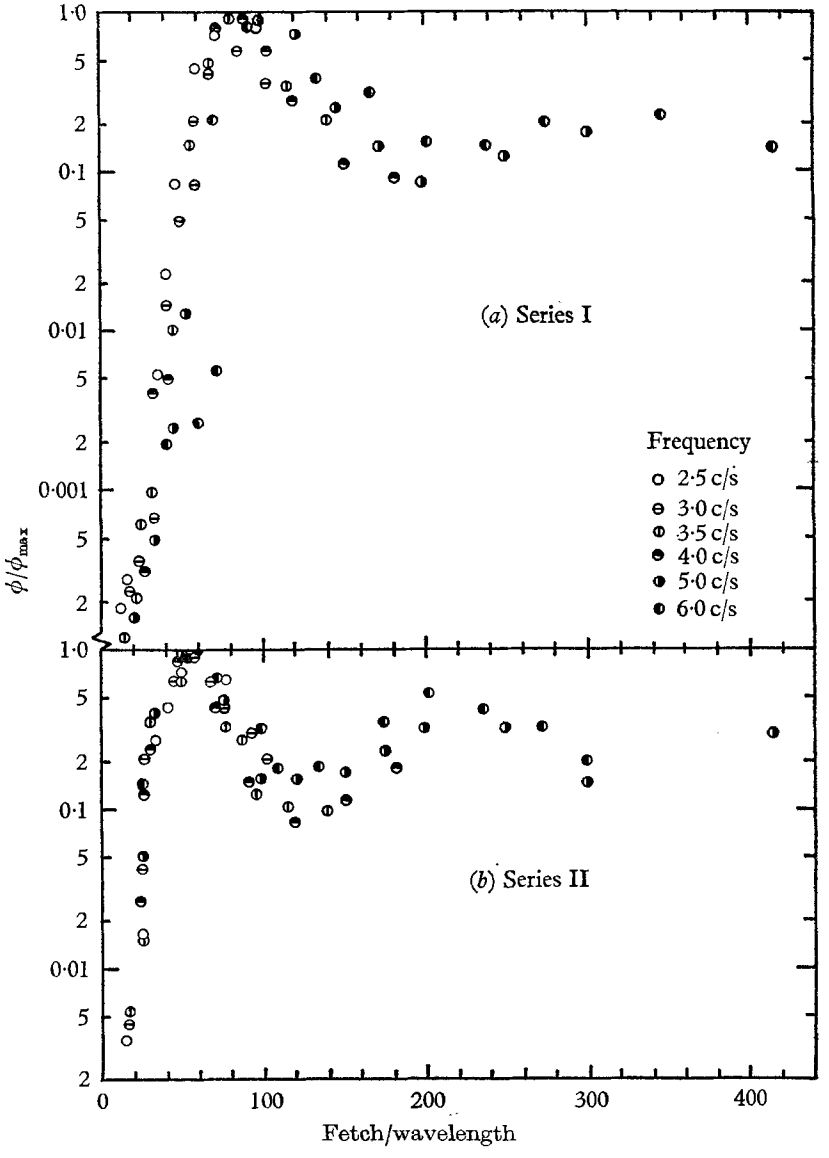

FIGURE 4. Normalized growth curves. Series I and II.

reached at a lower spectral density in these components; thus $\phi_{\max}$ decreases as σ increases. It is also apparent that the higher-frequency components have larger growth rates.

Normalized growth curves, shown in figure 4, seem to coalesce to form a band which has a peak at $\phi = \phi_{\max}$ and $F/\lambda = \tilde{F}/\lambda$. The band then decays and approaches an eventual equilibrium. This effect has also been observed in the

ocean by Barnett & Wilkerson (1967), who referred to it as an overshoot effect. The presence of the peak in the growth curves imposes an upper limit, with respect to fetch measured in wavelengths, upon the possible validity of Miles's (1962*a*) theory, which predicts exponential growth. Table 2 lists values of $\tilde{F}/\lambda$ for each series. Only those frequency components for which a definite first peak could be defined in their growth curve are listed. The $\tilde{F}/\lambda$ values are approximate because $\tilde{F}$ can be determined only to within $\pm 5\,\%$, its value depending upon just how the growth curve is passed through the data points (see figure 3). For

Frequency (c/s)	$\tilde{F}/\lambda$ Series I	Series II	Series III	Series IV
2·0			43·6	24·6
2·5		55·1	42·7	17·1
3·0	87·6	50·8	38·3	14·0
3·5	81·0	47·7	36·8	13·1
4·0	84·4	43·8	34·4	
5·0	87·7	48·7	33·1	
6·0	94·0	50·0		
Mean values	86·9	49·3	38·1	17·2

TABLE 2. Fetch, in wavelengths, at which growth curves reach their maximum value

series I and II, $\tilde{F}/\lambda$ first decreases with an increase in frequency, and then increases. There is a monotonic decrease of $\tilde{F}/\lambda$ as the frequency increases for series III and IV. From the present data it is thus not clear how $\tilde{F}/\lambda$ varies with frequency. The mean values given in the lowest line of table 3 can, with caution, be interpreted as upper limits for the corresponding wind velocity on the region of exponential growth in the Stanford facility. As one would expect, at higher wind speeds the limiting fetch for exponential growth is reduced.

For values of $4mF/c \ll 1$ theory predicts a region of linear growth. Figure 5 shows growth curves from series I for four different frequencies. Each shows an apparently linear portion and a transition to a steep region which is the start of exponential growth. The linear portion, which may or may not be present with $\sigma = 2{\cdot}5$ c/s, persists longer at the lower frequencies because these components grow less rapidly. Values of $4mF/c$, calculated using the fetch at which the lines start to curve, are noted on each plot and are all less than 1·0. One concludes that within the limits of the experimental accuracy there is a region of linear growth bounded from above by a value of $4mF/c$ which is less than 1·0. For all but the lowest wind speeds and the smallest frequencies this limit is exceeded almost immediately.

5.3. *Computations from theory*

Some typical growth rates, as predicted by Miles's (1962*a*) theory and computed according to the procedure outlined in § 4.2, are shown in table 3. Computations were done only for fetches less than that at which the particular component reached its maximum energy. Values of z, which must be appreciably less than

1 if the approximations made in deriving (1) are to be valid, are given for each case. The maximum value that occurred in the computations was 0·12.

The growth rates shown in column A, table 3, are those computed using (1) and reflect the change in growth rate with fetch. Those in column B have been computed from a mean value of U_* at a fetch in the centre of the straight portion

Frequency (c/s)	Fetch (ft.)	z	m sec^{-1}	Growth rates (ft.$^{-1}$) A	B	Expt.
			Series I (α = 6·0)			
2·5	5·0	0·12	0·038	0·105		
	9·1	0·12	0·039	0·067		
	19·1	0·11	0·042	0·047	0·045	0·075
	28·7	0·10	0·049	0·048		
	43·8	0·10	0·049	0·050		
3·0	5·0	0·11	0·092	0·143		
	9·1	0·11	0·094	0·113		
	19·1	0·10	0·100	0·111	0·105	0·090
	28·7	0·09	0·115	0·131		
	43·8	0·09	0·116	0·145		
3·5	5·0	0·11	0·193	0·250		
	9·1	0·11	0·196	0·243	0·241	0·170
	19·1	0·10	0·208	0·269		
	28·7	0·09	0·238	0·317		
4·0	5·0	0·10	0·362	0·499		
	9·1	0·10	0·368	0·518	0·513	0·222
	19·1	0·10	0·390	0·580		
	28·7	0·08	0·445	0·683		
5·0	5·0	0·10	1·03	1·72		
	9·1	9·10	1·04	1·79	1·70	0·370
	19·1	0·09	1·10	1·98		
			Series III (α = 8·0)			
2·0	5·0	0·05	0·051	0·106		
	9·1	0·05	0·054	0·069		
	19·1	0·05	0·055	0·048	0·042	0·119
	28·7	0·05	0·054	0·043		
	43·8	0·04	0·058	0·044		
2·5	5·0	0·05	0·148	0·166		
	9·1	0·04	0·156	0·144		
	19·1	0·04	0·159	0·141	0·135	0·175
	28·7	0·04	0·157	0·143		
	43·8	0·04	0·166	0·154		
3·0	5·0	0·04	0·353	0·366		
	9·1	0·04	0·371	0·381	0·375	0·244
	19·1	0·04	0·377	0·396		
3·5	5·0	0·04	0·74	0·879	0·913	0·278
	9·1	0·04	0·78	0·930		
4·0	5·0	0·04	1·40	1·89	1·87	0·270
	9·1	0·04	1·47	2·00		

TABLE 3. Growth rates

of the growth curve. Growth rates found from the slope of experimental growth curves are shown in the last column.

For small frequencies, the growth rates in column A first decrease with fetch and then increase. At higher frequencies the growth rates always increase with

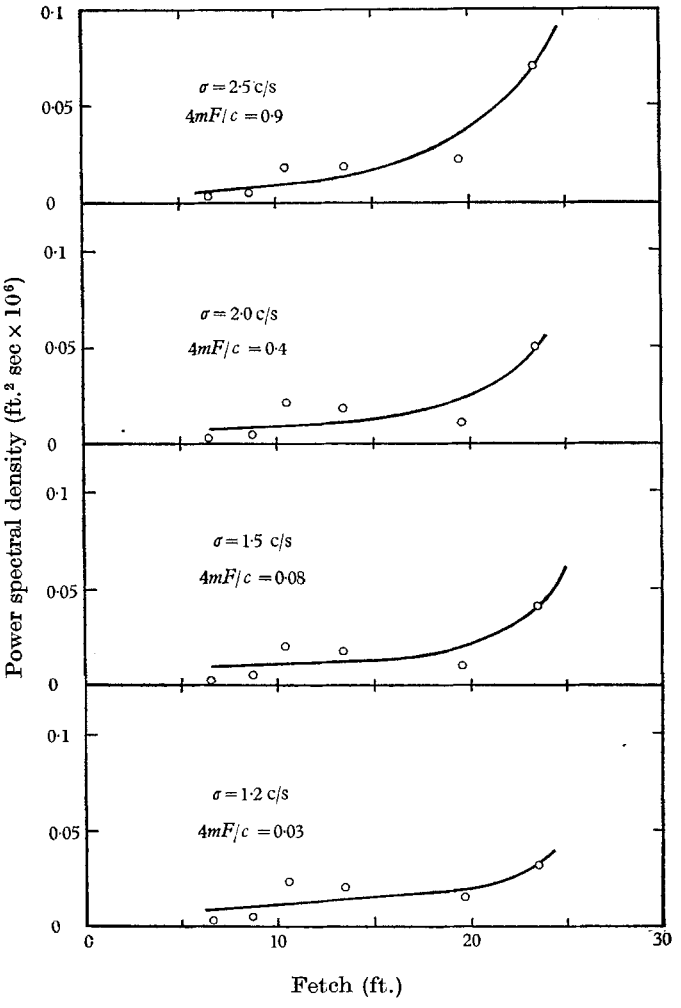

FIGURE 5. Growth of spectral components. Series I.

fetch. The explanation for this lies in the term $\exp(4mF/c)/(\exp(4mF/c) - 1)$, which decreases with an increase in $4mF/c$. When $4mF/c > 2$, however, the decrease is not sufficient to offset the effect of the term $\{m + F\,\partial m/\partial F\}$ which increases with fetch. Only low-frequency components have values of m small enough and values of c large enough to ensure that $4mF/c < 2$. Table 3 also shows that the predicted growth rate increases appreciably with increase in α and drastically with increase in frequency.

5.4. *Comparison of theory and experiment*

Qualitatively, in two aspects, there is agreement between the theoretical and the experimental growth rates. Both increase as the wave frequency increases and both increase with the wind velocity. However, the increase in the theoretical growth rate with fetch predicts growth curves which bend upwards rather than over as the experimental ones do. This increase is a direct result of the increase in m with fetch and suggests that it would probably be fruitless to devise a more elaborate scheme than the one used here to allow for the change in U_* with fetch.

For a constant value of α, table 3 shows that at each fetch growth rates of the low-frequency components in a wave train are under-predicted. For higher-frequency components the predicted growth rates exceed the experimental. Hence at each fetch, for a given α, there must be a frequency for which agreement between theory and experiment is best. This optimum frequency decreases with fetch for each value of α used in the computations.

Agreement between measured and predicted growth rates for all frequencies in a particular wave train can possibly be achieved by using smaller values of α for the higher frequencies. Since U_* is an average determined by all the wave components comprising the water surface it cannot be associated with any single frequency. Physically then, if α is to depend on wave frequency, U_1 must also be a function of frequency. In flow over water waves it is doubtful whether a true sublayer exists; if it does not U_1 becomes simply a reference velocity. As such it should be determined by the velocity profile and thus, like U_*, not related to any one wave component. One concludes that α is dependent on the water surface as a whole and must be independent of any particular wave frequency. Hence when a spectrum of waves is involved the theory must be considered inadequate for predicting growth rates over any significant portion of the spectrum.

For a simple wave form it should be possible to match theory and experiment by adjusting the value of α. The present results show that for frequencies greater than 3·5 c/s very low values of α are required. A computation with $\alpha = 4{\cdot}0$, however, did not reduce the predicted growth rates sufficiently and smaller values of α are unrealistic since for a smooth flat plate $\alpha = 6{\cdot}6$. The theory is thus applicable only for simple waves of low frequency.

Possible variation of α with fetch has not been accounted for in the derivation of (4). Since α cannot be determined from experimental data it appears to be impossible to evaluate the derivative $\partial\alpha/\partial F$ by any means other than a comparison of predicted and measured growth rates. But to do this would invalidate any evaluation of Miles's (1962*a*) theory. However, U_* does vary with fetch and it is also probable that U_1 varies with fetch. Therefore α may be expected to be fetch dependent. The experiments suggest that α should be reduced as the fetch increases. This would offset the increase in growth rate factor m and possibly permit the correct prediction of the growth rate to the fetch at which $\phi = \phi_{\max}$.

The above trends are illustrated in figures 6 and 7. Experimental points are shown and lines with the predicted slope have been drawn in. These lines were

placed so that they would intersect the growth curve (the dashed line) at the fetch for which their slope was computed. Only low frequencies have been considered since the agreement is so poor at high frequencies. The upper half of figure

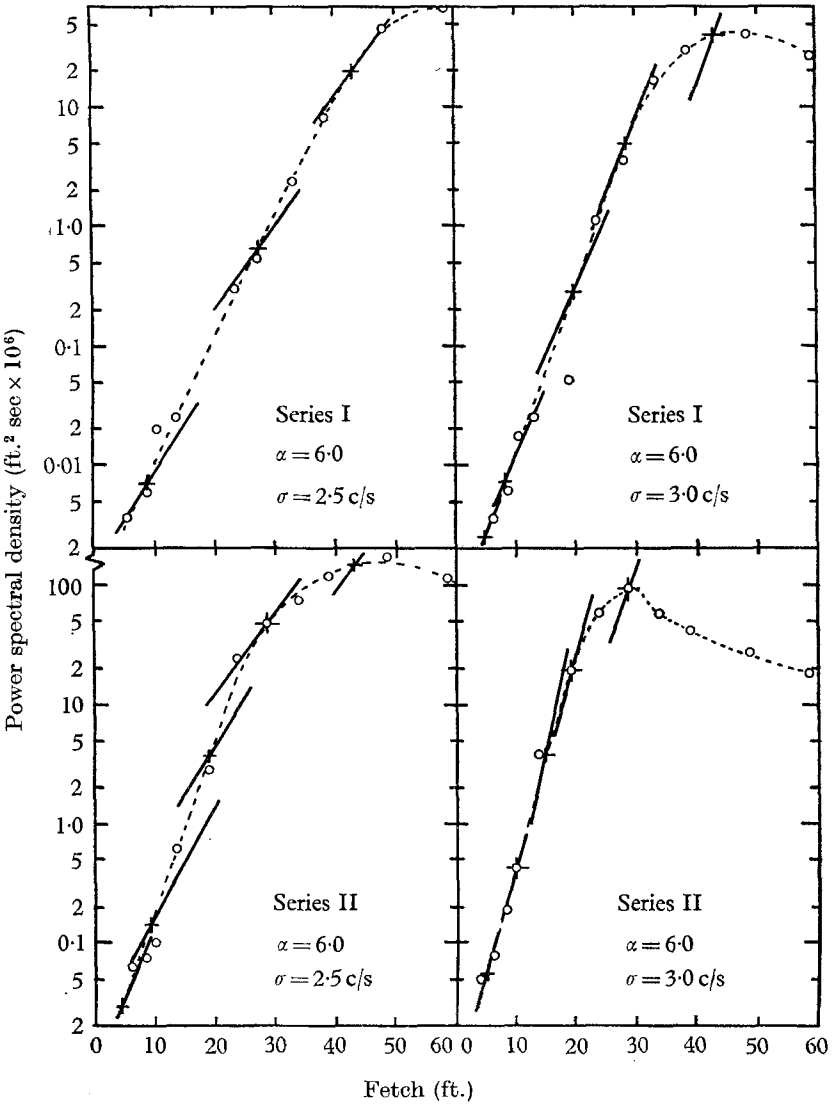

FIGURE 6. Predicted slopes and experimental data. Series I and II.

6 shows results from series I with $\alpha = 6{\cdot}0$. Both examples show an initial decrease of slope with fetch and then an increase. For 2·5 c/s the theory under-predicts except at a fetch of 40 ft. At the higher frequency the agreement is very good. This is evidently the frequency for best agreement with $\alpha = 6{\cdot}0$ and the U_* of series I. The same trends are seen in the lower half of figure 6, which refers to series II. The optimum frequency would seem to be less than 3·0 c/s since the

theory over-predicts this case for all except the short fetch. Similar remarks can be made about figure 7, where $\alpha = 10$. The optimum frequency seems to be 2·5 c/s for series III and somewhat less than this at the higher U_* of series IV.

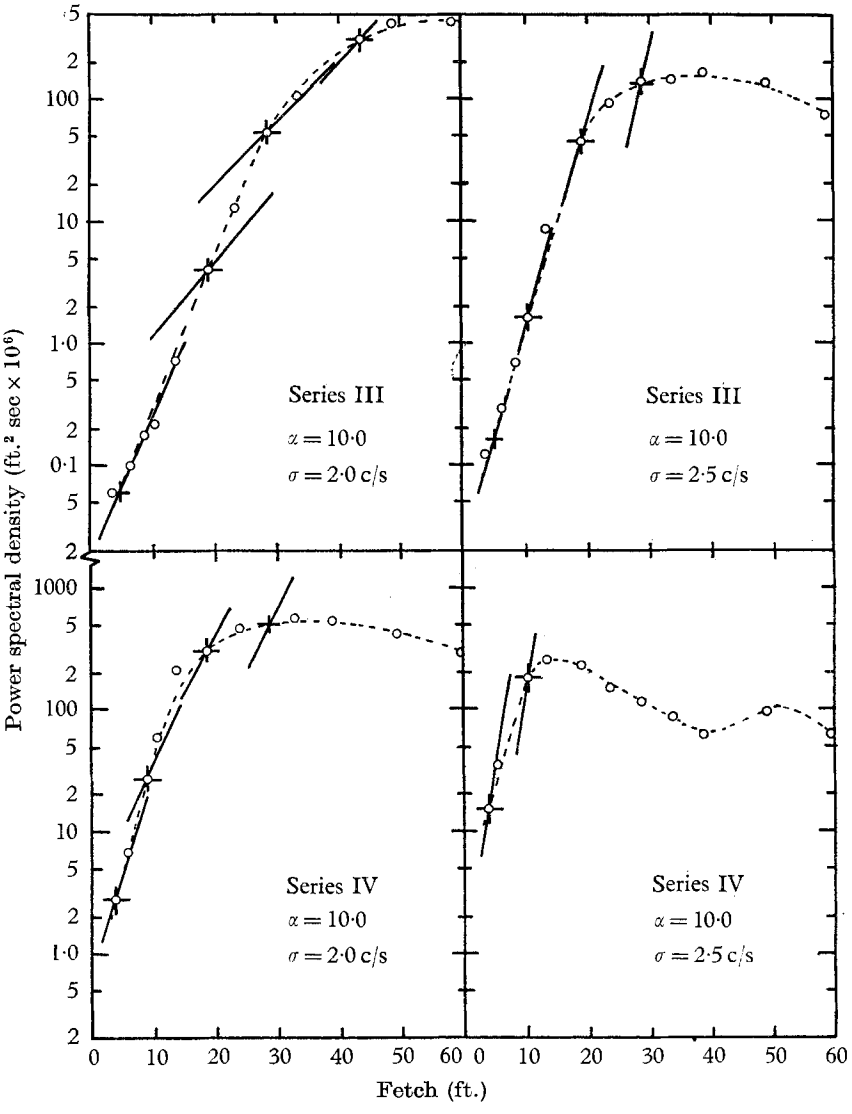

FIGURE 7. Predicted slopes and experimental data. Series III and IV.

6. Summary

A laboratory investigation has been made of the response of a water surface under the action of wind. From measured spectra of water surface displacement, growth curves for different frequency components in the generated wave train were drawn. Growth curves for the higher-frequency components (3–6 c/s) reached a maximum at fetches less than the length of the test section. When

plotted in the form $\log(\phi/\phi_{\max})$ against F/λ the data displayed an overshoot phenomenon by defining a band that rose steeply to a maximum, decreased and then oscillated about a final value of $\phi/\phi_{\max} = \phi_e$. The value of ϕ_e depended upon the air velocity, increasing from 0·17 in series I to 0·5 in series IV. An upper bound to the exponential growth region for a given wind condition was given by the F/λ value at which $\phi = \phi_{\max}$. A lower bound was found to depend upon the parameter $4mF/c$. In most instances this lower bound was exceeded immediately.

Experimental growth rates were compared with those predicted by the viscous Reynolds stress theory proposed by Miles (1962*a*). The theory assumed the air-velocity profile to be linear near the water surface and to be asymptotically logarithmic. The experimental profile deviated slightly from logarithmic and it is unlikely that a viscous sublayer existed. This difference in profile shape meant not only was there some uncertainty in the value of U_*, but also the reference velocity U_1, defined by Miles to be the velocity at the edge of the viscous sublayer, could not be determined experimentally. In part, these difficulties were overcome by introducing the parameter $\alpha = U_1/U_*$ and selecting its value to give best possible agreement between theory and experiment. Good agreement was obtained, with values of α in the range suggested by Miles (1962*a*), for wave frequencies less than 3·5 c/s. No agreement between the predicted and measured growth rates could be found for the higher frequencies.

Agreement for all frequencies in a wave train was possible only if α was decreased for the higher frequencies. That α should depend on frequency is inconsistent with its definition as the ratio of two velocities each of which is determined by the velocity profile. The viscous Reynolds stress theory is thus inadequate for predicting growth rates in situations where a spectrum of waves is involved.

Financial support for this investigation was provided by the Office of Naval Research through Contract Nonr 225(71) and the National Science Foundation by Grant NSF GK 736.

REFERENCES

BARNETT, T. P. & WILKERSON, J. G. 1967 On the generation of wind waves as inferred from airborne radar measurements of fetch-limited spectra. *J. Mar. Res.* **25** (3), 292–328.

BENJAMIN, T. B. 1959 Shearing flow over a wavy boundary. *J. Fluid Mech.* **6**, 161–205.

BLACKMAN, R. B. & TUKEY, J. W. 1959 *The Measurement of Power Spectra from the Point of View of Communications Engineering*. New York: Dover.

HIDY, G. M. & PLATE, E. J. 1966 Wind action on water standing in a laboratory wave channel. *J. Fluid Mech.* **26**, 651–687.

MILES, J. W. 1957 On the generation of surface waves by shear flows. *J. Fluid Mech.* **3**, 185–204.

MILES, J. W. 1959 On the generation of surface waves by shear flows. Part 2. *J. Fluid Mech.* **6**, 568–582.

MILES, J. W. 1960 On the generation of surface waves by turbulent shear flows. *J. Fluid Mech.* **7**, 469–478.

MILES, J. W. 1962*a* On the generation of surface waves by shear flows. Part 4. *J. Fluid Mech.* **13**, 433–448.

MILES, J. W. 1962*b* A note on the inviscid Orr–Sommerfeld equation. *J. Fluid Mech.* **13**, 427–432.

PHILLIPS, O. M. 1957 On the generation of waves by turbulent wind. *J. Fluid Mech.* **2**, 417–445.

PHILLIPS, O. M. 1966 *The Dynamics of the Upper Ocean.* Cambridge University Press.

SHEMDIN, O. H. 1967 Experimental and analytical investigation of the air velocity profile above progressive waves. Stanford University, *Dept of Civil Engng Tech. Rept* no. 82, Stanford.

SUTHERLAND, A. J. 1967 Spectral measurements and growth rates of wind generated water waves. Stanford University, *Dept of Civil Engng Tech. Rept.* no. 84, Stanford.